

AECL-6484

ATOMIC ENERGY
OF CANADA LIMITED



L'ÉNERGIE ATOMIQUE
DU CANADA LIMITÉE

**MEASUREMENTS OF THE
RELATIVE ANGULAR EFFICIENCY OF A Ge(Li) DETECTOR:
Q_k FACTORS AND DOPPLER BROADENING**

**Mesure de l'efficacité
angulaire relative d'un détecteur au Ge(Li):
facteurs Q_k et élargissement Doppler**

T.K. ALEXANDER, J.S. FORSTER, G.C. BALL and W.G. DAVIES

Chalk River Nuclear Laboratories

Laboratoires nucléaires de Chalk River

Chalk River, Ontario

February 1979 février

ATOMIC ENERGY OF CANADA LIMITED

MEASUREMENTS OF THE RELATIVE ANGULAR EFFICIENCY
OF A Ge(Li) DETECTOR: Q_k FACTORS AND DOPPLER BROADENING

by

T.K. Alexander, J.S. Forster, G.C. Ball and W.G. Davies

Nuclear Physics Branch
Chalk River Nuclear Laboratories
Chalk River, Ontario KOJ 1J0
February 1979

AECL-6484

Mesure de l'efficacité angulaire relative d'un
détecteur au Ge(Li): facteurs Q_k et élargissement Doppler

par

T.K. Alexander, J.S. Forster, G.C. Ball et W.G. Davies

Résumé

On a mesuré l'efficacité relative d'un détecteur cylindrique au lithium-germanium en fonction de l'angle d'incidence et de l'énergie des rayons gamma (660, 898, 1369, 1836 et 2754 keV), pour trois distances source-détecteur (4.6, 8 et 10 cm entre la source et la face avant du récipient contenant le détecteur). On se sert des données ainsi obtenues pour calculer la valeur des facteurs d'atténuation, Q_k , employés dans les analyses de répartition angulaire et pour calculer l'élargissement Doppler provoqué par l'angle solide fini du détecteur sous-tendu à la source en mouvement.

L'Energie Atomique du Canada, Limitée
Laboratoires nucléaires de Chalk River
Chalk River, Ontario

Février 1979

MEASUREMENTS OF THE RELATIVE ANGULAR EFFICIENCY
OF A Ge(Li) DETECTOR: Q_k FACTORS AND DOPPLER BROADENING

by

T.K. Alexander, J.S. Forster, G.C. Ball and W.G. Davies

ABSTRACT

The relative efficiency of a cylindrical Ge(Li) detector has been measured as a function of the angle of incidence and the energy of the gamma rays (660, 898, 1369, 1836 and 2754 keV), for three source-to-detector distances (4.6, 8 and 10 cm between the source and the front face of the detector container). These data are used to calculate values of the attenuation factors, Q_k , for use in angular distribution analysis and to calculate the Doppler broadening arising from the finite solid angle of the detector subtended to a moving source.

Nuclear Physics Branch
Chalk River Nuclear Laboratories
February 1979

AECL-6484

CONTENTS

	<u>Page</u>
ABSTRACT	ii
1. INTRODUCTION	1
2. MEASUREMENTS	2
3. RESULTS	3
3.1 Relative Efficiency versus Angle Curves	3
3.2 Attenuation Coefficients	4
3.3 Doppler Broadening	5
ACKNOWLEDGEMENTS	7
REFERENCES	8
FIGURE CAPTIONS	9
TABLE 1	10
FIGURES	11 - 17

1. INTRODUCTION

The Doppler broadening resulting from the spread in angle subtended by a gamma-ray detector can sometimes be larger than the intrinsic resolution of a Ge(Li) detector. In the analysis of gamma-ray Doppler-broadened lineshapes to obtain lifetimes of nuclear levels, the effect of the solid angle Doppler broadening must be known. Clearly the solid angle broadening is smallest when the detector is located at 0° with respect to the velocity vector of the radiating nuclei. If the experimental objective is to minimize the Doppler broadening and obtain the best possible resolution rather than lifetime information, then the recoiling nuclei should not change velocity during their lifetime.

The Doppler broadening can be calculated in a straightforward manner provided the efficiency of the Ge(Li) detector is known as a function of the angle of incidence, gamma-ray energy and source-to-detector distance. In this paper, measurements of the relative efficiency of a Ge(Li) detector for five gamma-ray energies and three source-to-detector distances are presented. The collimated sources were located on the axis of symmetry of the cylindrical detector and rotated to scan the detector radially. The results are used to calculate the Doppler broadening discussed above for different target-to-detector distances and different gamma-ray energies. The results are also used to calculate the attenuation coefficients, Q_k ,⁽¹⁾ of the Legendre polynomials $P_k(\cos \theta)$ useful for interpreting angular distribution measurements.

There appears to be few published measurements⁽²⁾ of the angular efficiency response of Ge(Li) detectors. The Q_k coefficients^(3,4,5) and the Doppler broadening effects⁽⁶⁾ are often estimated by calculating the angular efficiency of the detector from its dimensions and known gamma-ray absorption coefficients.

In some instances, calculated values are adequate for interpreting measurements; but in others better accuracy is required.

2. MEASUREMENTS

Figure 1 is a schematic diagram of the apparatus used to measure the relative angular efficiency of a Ge(Li) detector. The detector (PGT VIII) is a true coaxial, cylindrical detector with the dimensions shown in Figure 1. These are: length = 47 mm, distance between the front face of the detector and the front face of the cryostat = 6,5 mm, crystal diameter = 53.5 mm and dead core diameter \sim 10 mm.

As shown in the figure, the source of gamma rays was placed at one end of a lead collimator which was 140 mm long and 5 mm in diameter, giving a beam with an angular divergence of 2° fwhm*. The collimator was placed on a rotatable carriage and the end of the collimator was at the centre of rotation. The symmetry axis of the detector was aligned with the collimator hole when it was at 0° . The distance between the collimator end and the detector face, D, was changed by moving the detector radially.

The angle, θ , of the collimator relative to the axis of the detector was changed under computer control, so that the relative efficiency scans of the detector were controlled automatically by the PDP-1 computer. The computer program moved the collimator to a new angle, accumulated a spectrum from the source for a specified length of time, and then wrote the spectrum as well as the elapsed time onto magnetic tape. The latter was useful for correcting the decay of the source intensity if the source was short lived. Usually the angular range

* full width at half maximum

covered both positive and negative angles beyond the maximum angle subtended by the detector. The magnetic tape data were later analyzed and the relative intensities of specific full-energy gamma-ray peaks were obtained as a function of angle for the detector at a given distance. Measurements using each source were done at three distances, $D = 4.6, 8$ and 10 cm. The sources (E_γ) used were ^{137}Cs (660 keV), ^{88}Y (898 and 1836 keV) and ^{24}Na (1369 and 2754 keV).

3. RESULTS

3.1 Relative Efficiency versus Angle Curves

Figure 2 shows some of the data obtained from the ^{137}Cs and ^{24}Na sources. For the 660 and 2754 keV gamma rays, the relative counts are shown as a function of angle for two distances, $D = 4.6$ and 10 cm. The experimental points are shown as crosses with uncertainty bars. The solid lines in the figure are the relative efficiencies calculated with the crystal dimensions shown in Figure 1 and the total absorption coefficients for the gamma-rays involved. The finite emittance of the collimator beam is small and was neglected in these calculations. It is seen that in general the calculated curve has a similar shape, but is too wide. If the outer radius of the detector is assumed to be about 2 to 3 mm smaller than it is specified to be, the agreement in width would be much better. In detail, the experimental data differ from the simple calculation which only applies to total absorption and does not apply to the full-energy peak of the gamma-ray. The peak efficiency has contributions from secondary interactions whose influence depends strongly on edge effects.

A reasonable approximation to the measurements in Figure 2 is to assume the efficiency curve is two Gaussians centered at $+\theta_m$ and $-\theta_m$ with width parameters σ , i.e. for $\theta \geq 0$

$$\epsilon(\theta) = K \exp \left\{ -(\theta - \theta_m)^2 / 2\sigma^2 \right\}$$

It can be seen in Figure 2 (a) and (c) that the data obtained at $D = 4.6$ cm would be better represented by a skewed Gaussian, but for the data at larger distances, Figure 2 (b) and (d), the Gaussian becomes a reasonable approximation.

In table 1, the measurements have been summarized in terms of the parameters θ_m and σ . This parameterization, although only approximate, is quite useful since it gives the general features of the measurements. The outer edges and widths of the distributions are well represented. These are the most important features.

3.2 Attenuation Coefficients

Also listed in table 1 are the attenuation coefficients Q_k for $k = 1, 2, 3$ and 4 which have been calculated from the experimental data. The values of Q_k have been obtained by evaluating the following expression,

$$Z_k = \frac{\int \epsilon(\theta) \cos^k \theta \sin \theta d\theta}{\int \epsilon(\theta) \sin \theta d\theta}$$

where $\epsilon(\theta)$ is the measured efficiency curve obtained from the data of Figure 2 with a background subtracted when necessary. The Q_k are then given by:

$$\begin{aligned} Q_1 &= Z_1 \\ Q_2 &= 1.5 Z_1 - 0.5 \\ Q_3 &= 2.5 Z_3 - 1.5 Z_1 \\ Q_4 &= (35/8) Z_4 - (30/8) Z_2 + 3/8 \end{aligned}$$

If the Gaussian shape approximation for $\epsilon(\theta)$ is used the values of Q_4 agree with the values listed in table 1 to better than 3% and with Q_2 to better than 1%.

The values of Q_2 and Q_4 as a function of the energy of the gamma rays are plotted in Figure 3 for the distance $D = 4.6$ cm. For comparison the values obtained by using the calculated efficiencies are shown as solid lines. The efficiencies correspond to those shown as the solid lines in Figure 2 where $R_2 = 2.68$ cm is the outer radius of the crystal. Also shown as a broken line are the calculated values for $R_2 = 2.50$ cm. The values of Q_2 and Q_4 derived from the experimental and calculated relative angular efficiencies for $D = 8$ and 10 cm are shown in Figure 4 (a) and Figure 4 (b) respectively. A more sophisticated calculation⁽⁷⁾ of the relative angular efficiencies should give Q_k values in better agreement with the experimental values without adjusting the crystal dimension arbitrarily.

3.3 Doppler Broadening

The Doppler broadened spectrum of gamma rays obtained with a detector located at 0° with respect to the recoil direction of the decaying nuclei can be calculated from the measured efficiency curves by using the relativistic Doppler formula and the aberration effect (see e.g. ref. 8).

If there are N nuclei decaying at velocity βc , then the number detected between angle θ and $\theta + d\theta$ is

$$N \cdot W(\theta_s) \cdot \epsilon(E_\gamma, \theta, D) \cdot \frac{d\Omega}{d\Omega_{lab}} \cdot 2\pi \sin\theta d\theta$$

where $W(\theta_s)$ = the angular distribution of the gamma rays in the moving frame.

$$\cos\theta = (\cos\theta_s + \beta) / (1 + \beta\cos\theta_s)$$

θ = laboratory angle

$\epsilon(E_\gamma, \theta, D)$ = the efficiency of the detector

$d\Omega$ = moving frame elemental solid angle

$d\Omega_{lab}$ = laboratory elemental solid angle

The energies of the gamma rays are

$$E_{\gamma}(\theta, \beta) = \frac{E_{\gamma}^0 \sqrt{1-\beta^2}}{1-\beta \cos \theta}$$

The efficiency function is given by the measurements for E_{γ}^0 . To take into account that the efficiency varies with E_{γ}^{-1} , then

$$\epsilon(E_{\gamma}, \theta, D) = \epsilon(E_{\gamma}^0, \theta, D) \cdot \frac{E_{\gamma}^0}{E_{\gamma}(\theta, \beta)}$$

The change of the solid angle resulting from the aberration is

$$\frac{d\Omega}{d\Omega_{\text{lab}}} = \frac{1-\beta^2}{(1-\beta \cos \theta)^2}$$

From these relations, the energy spectrum calculated when $\beta > 0$ is

$$N(E_{\gamma}) dE_{\gamma} = 2\pi N \cdot W(\theta_s) \cdot \epsilon(E_{\gamma}^0, \theta, D) \cdot \frac{\sqrt{1-\beta^2}}{\beta} \frac{dE_{\gamma}}{E_{\gamma}}$$

The intrinsic lineshape of the Ge(Li) detector is assumed to be a Gaussian, and this is folded with $N(E_{\gamma})$ to give the actual spectrum.

In Fig. 5 the calculated Doppler broadened lineshapes for the 2754 keV gamma ray are shown for $D = 4.6$ and 10 cm and for $\beta = 0.05$ and 0.10 . The shapes were calculated by using the measured values of $\epsilon(E_{\gamma}^0, \theta, D)$ and $W(\theta_s)$ was assumed to be isotropic. All lineshapes are normalized to have equal intensity. The shape shown for $\beta = 0$ is a Gaussian intrinsic shape with the full width at half maximum (fwhm) equal to 3 keV. It can be seen that the Doppler broadening is large compared to the intrinsic resolution, especially for $D = 4.6$ cm. For $\beta = 0.05$, the fwhm equals 7.5 keV and for $\beta = 0.10$, the fwhm equals 16 keV when $D = 4.6$ cm.

In Fig. 6 and 7, similar calculations are shown for the 1369 and 660 keV gamma rays.

The calculation shown in Fig. 5, 6 and 7 used the experimental efficiency curves directly but the parameterization in terms of the Gaussian parameters given in Table 1 yields shapes closely approximating those in the figures. For the purpose of analyzing Doppler broadened lineshapes to obtain nuclear lifetime measurements, the Gaussian approximation has been used and reproduces the experimental lineshapes well.⁽⁹⁾ It should be added, that if the calculated efficiency curves shown as the solid lines in Fig. 2 are used, the calculated lineshapes do not reproduce the experimental shapes very well and the analysis yields incorrect lifetime values when the lifetimes are short (< 100 fs).

Acknowledgements

We would like to thank J.S. Merritt for preparing the ^{24}Na and ^{88}Y sources and M.L. Delaney for help in the data analysis.

We would also like to thank R.B. Walker for designing an angular distribution table used in adjusting the collimator relative to the detector.

References

1. M.E. Rose, Phys. Rev. 91 (1953) 610.
2. R.G. Arns, S.E. Caldwell and W.G. Monahan, Nucl. Instr. & Methods 78 (1970) 295.
3. R. Griffiths, Oxford University Nuclear Physics Laboratory Report 1/71, 1971 and references therein.
4. A. Roy and K.V.K. Iyengar, Nucl. Instr. and Methods 114 (1974) 29 and references therein.
5. K.S. Krane, Nucl. Instr. and Methods 98 (1972) 205 and references therein.
6. see e.g. J.A.J. Hermans, G.A.P. Engelbertink, M.A. Van Driel, H.H. Eggenhuisen and D. Bucurescu, Nucl. Phys. A255 (1975) 221.
7. M.J.L. Yates in "Alpha-, beta and gamma ray Spectroscopy, ed. K. Siegbahn, North-Holland Publishing Co. Amsterdam, 1965. and Nucl. Instr. and Methods 23 (1963), 152.
8. T.K. Alexander and J.S. Forster, in Advances in Nuclear Physics Vol. 10, ed. M. Baranger and E. Vogt, Plenum Press, New York and London, 1978, p. 197-331.
9. T.K. Alexander, G.C. Ball, W.G. Davies and J.S. Forster, to be published in Nuclear Physics.

Figures

Fig. 1: A schematic diagram of the apparatus, showing the collimator and detector dimensions.

Fig. 2: The relative number of counts detected as a function of the angle of the collimator for

- a) The 660 keV γ -ray from ^{137}Cs at $D = 4.6$ cm
- b) " " " " " at $D = 10$ cm
- c) The 2754 keV γ -ray from ^{24}Na at $D = 4.6$ cm
- d) " " " " " at $D = 10$ cm

The solid lines are calculated using total absorption coefficients and the dimensions of the crystal.

Fig. 3: The values of Q_2 and Q_4 for $D = 4.6$ cm as a function of the gamma ray energy E_γ . Experimental values are shown as dots with uncertainty bars determined from counting statistics only. The full and dashed lines were calculated using the crystal dimensions indicated. The specified crystal outer radius is $R_2 = 2.68$ cm.

Fig. 4: a) The values of Q_2 and Q_4 for $D = 8$ cm
b) The values of Q_2 and Q_4 for $D = 10$ cm
See Fig. 3 caption for further details.

Fig. 5: The Doppler broadened spectrum shapes calculated from the measured efficiency curves for 2754 keV gamma rays from a source with velocities $\beta = 0, 0.05$ and 0.1 at distances $D = 4.6$ cm (solid lines) and $D = 10$ cm (dashed lines). The energy increment scale has an arbitrary zero for each β .

Fig. 6: The calculated Doppler broadened spectrum shapes for 1369 keV gamma rays. See Fig. 5 caption for further details.

Fig. 7: The calculated Doppler broadened spectrum shapes for 660 keV gamma rays. See Fig. 5 caption for further details.

Table 1
Summary of Results

E (MeV)	D (cm)	θ_m (deg)	σ (deg)	Q_1	Q_2	Q_3	Q_4
0.66	4.6	(12.23	5.12) ^{a)}	0.966 (1) ^{b)}	0.900 (2)	0.807 (4)	0.694 (7)
	8.0	(7.82	3.86)	0.985 (2)	0.956 (3)	0.913 (5)	0.857 (10)
	10.0	(6.30	3.26)	0.989 (2)	0.968 (3)	0.937 (6)	0.896 (11)
0.898	4.6	(11.28	5.73)	0.969 (2)	0.910 (3)	0.826 (5)	0.722 (10)
	8.0	(7.30	4.31)	0.986 (2)	0.957 (3)	0.916 (6)	0.863 (12)
	10.0	(7.23	4.10)	0.987 (2)	0.961 (3)	0.924 (6)	0.876 (12)
1.369	4.6	11.58	5.80	0.966 (1)	0.900 (1)	0.807 (1)	0.695 (2)
	8.0	7.63	4.04	0.984 (1)	0.954 (1)	0.909 (2)	0.852 (3)
	10.0	6.24	3.41	0.989 (1)	0.967 (2)	0.934 (3)	0.892 (7)
1.836	4.6	10.50	6.78	0.965 (2)	0.897 (2)	0.802 (5)	0.687 (9)
	8.0	6.88	4.94	0.983 (2)	0.949 (3)	0.900 (6)	0.838 (11)
	10.0	5.99	4.13	0.986 (2)	0.960 (3)	0.921 (6)	0.871 (12)
2.754	4.6	11.15	5.95	0.966 (1)	0.902 (1)	0.811 (2)	0.701 (4)
	8.0	7.35	4.16	0.984 (1)	0.953 (1)	0.908 (3)	0.850 (5)
	10.0	6.17	3.62	0.988 (2)	0.964 (2)	0.930 (4)	0.885 (9)

a) - bracketed values are the results of a fit where the data are not well approximated by a Gaussian.

b) - 0.966 (1) means 0.966 ± 0.001 where the error is from the counting statistics only.

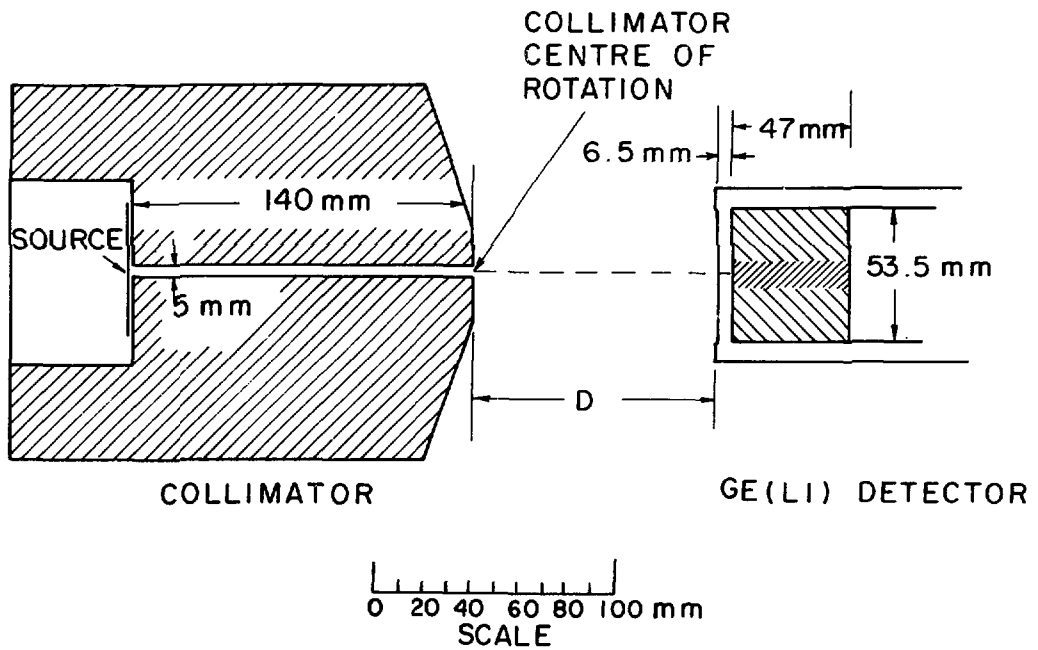


Figure 1

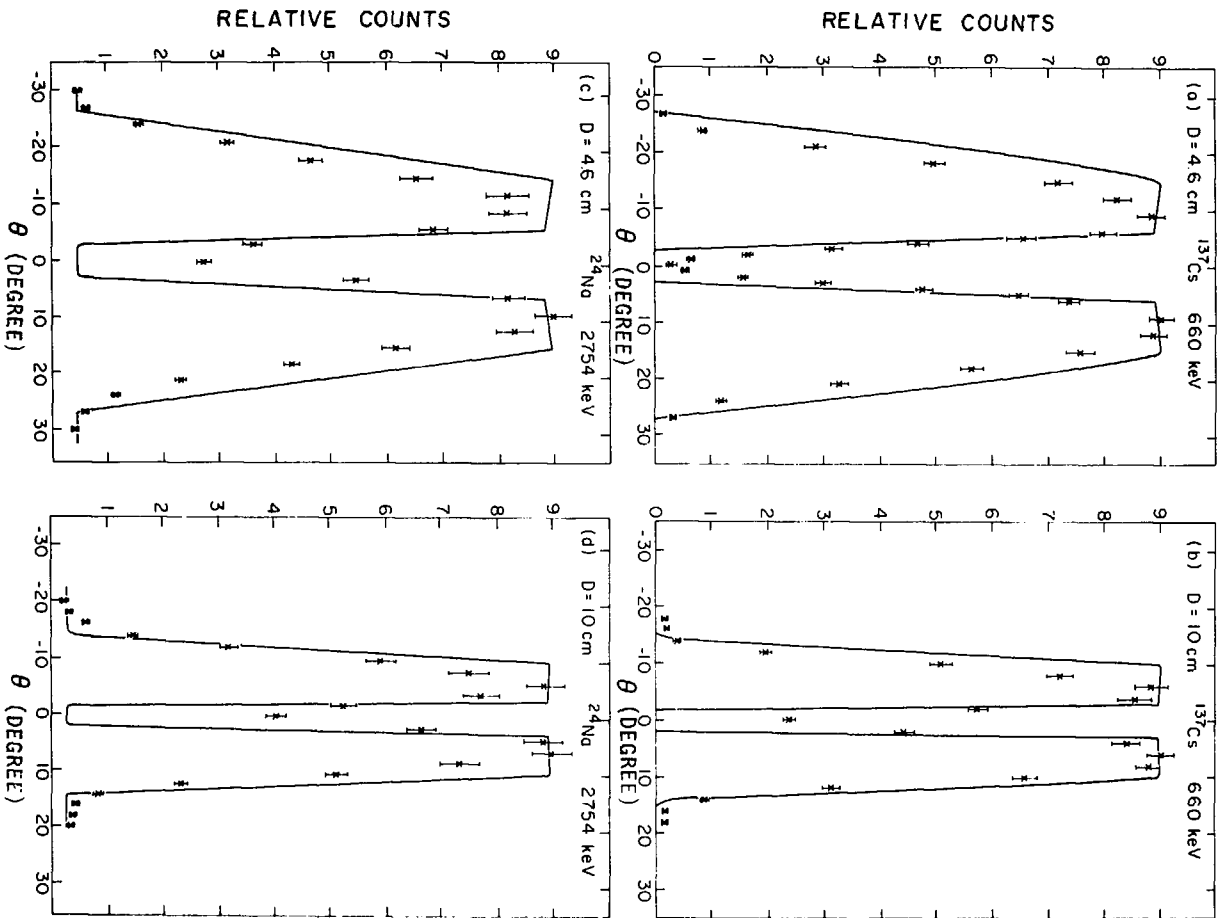


Figure 2

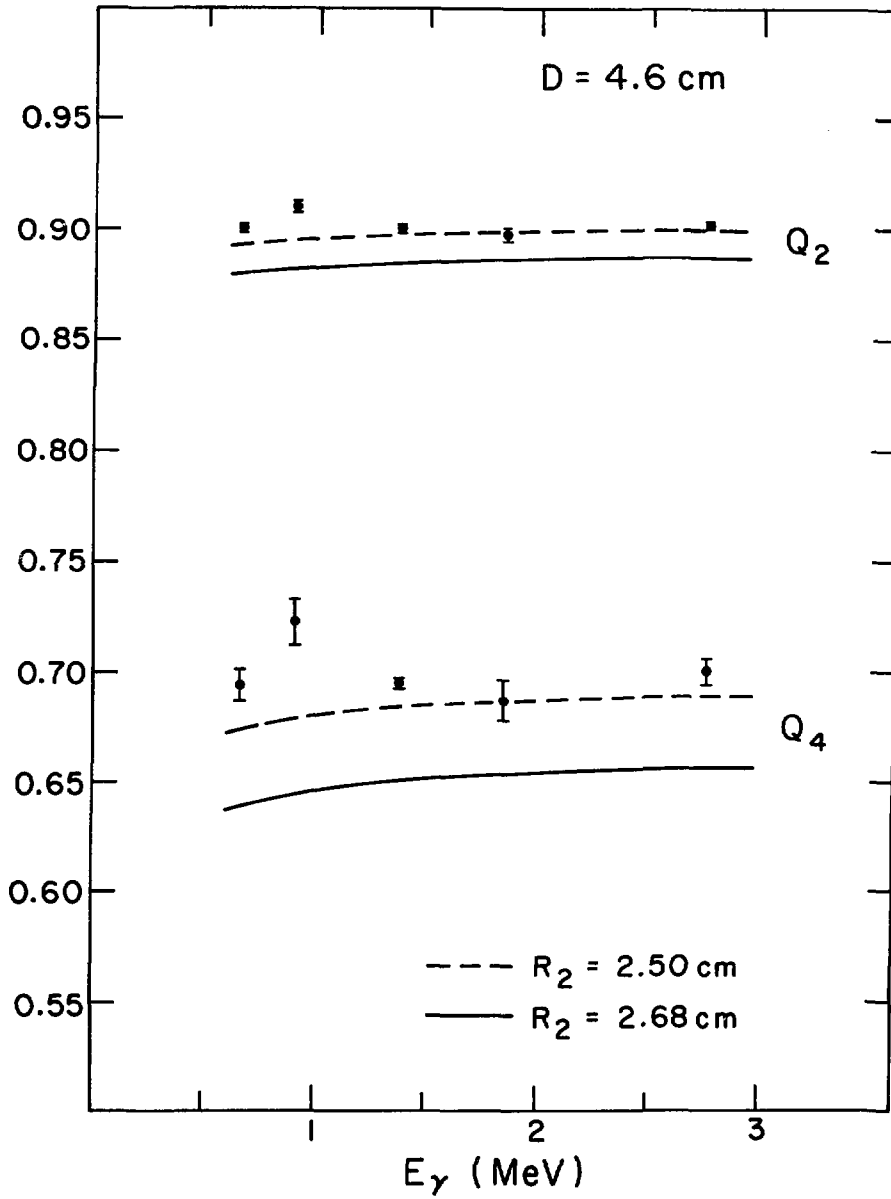


Figure 3

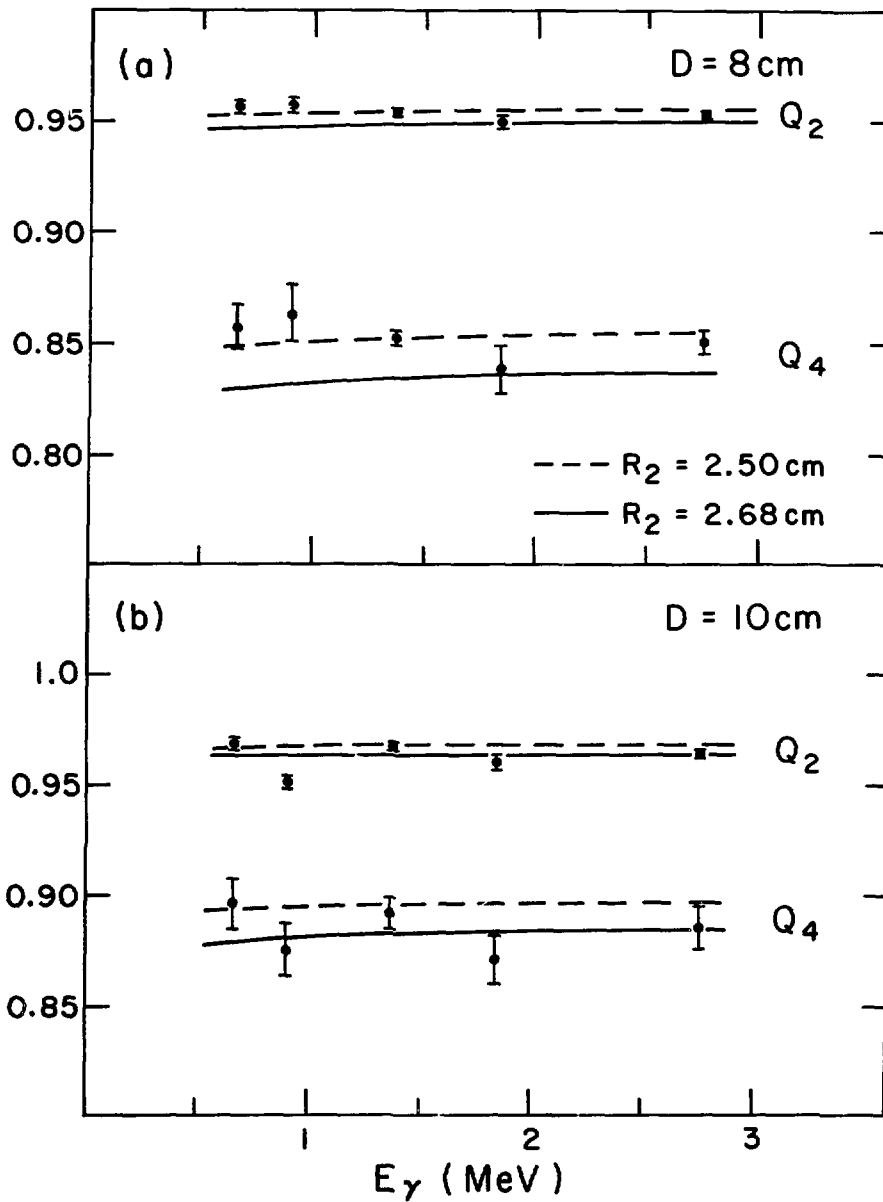


Figure 4

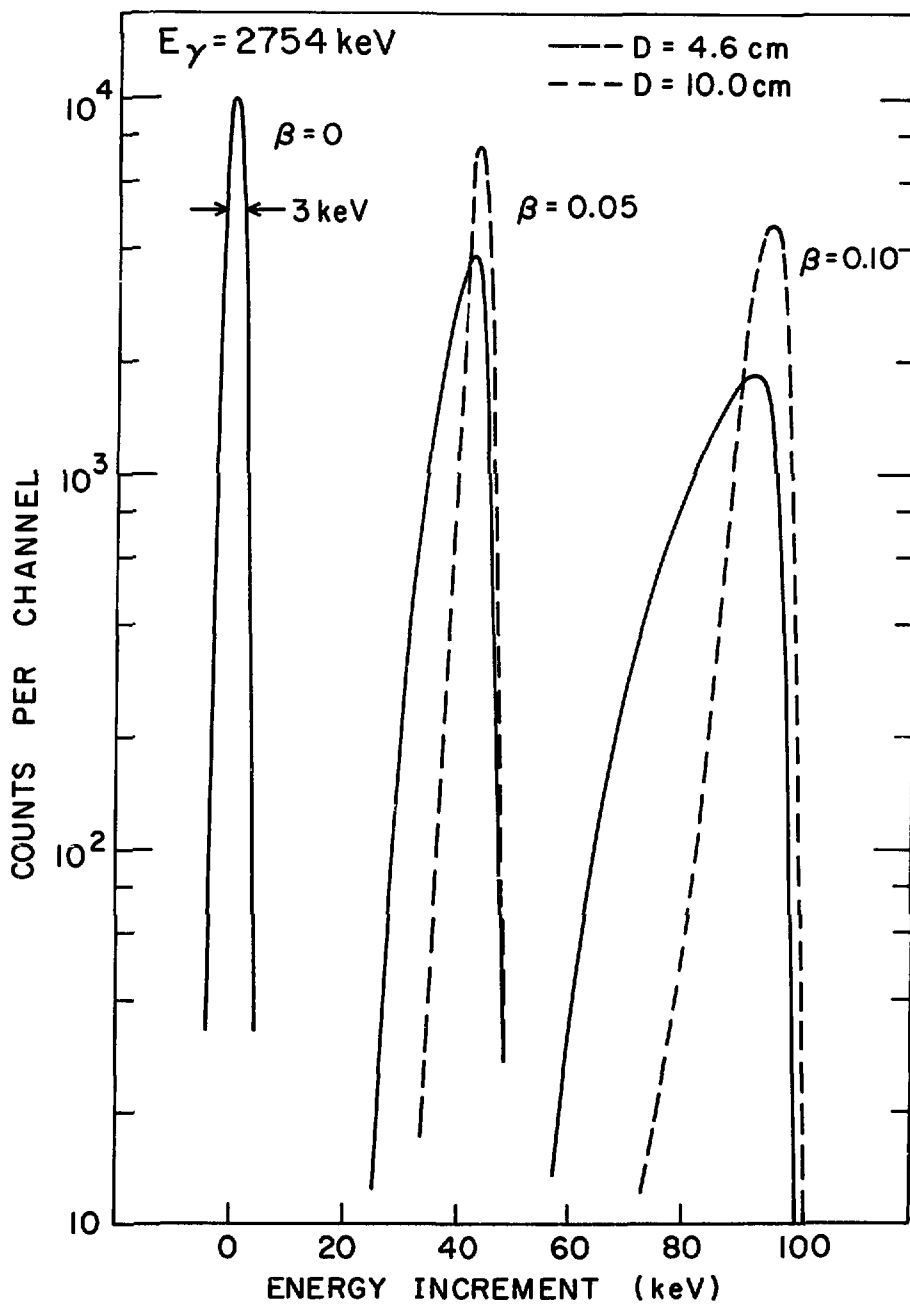


Figure 5

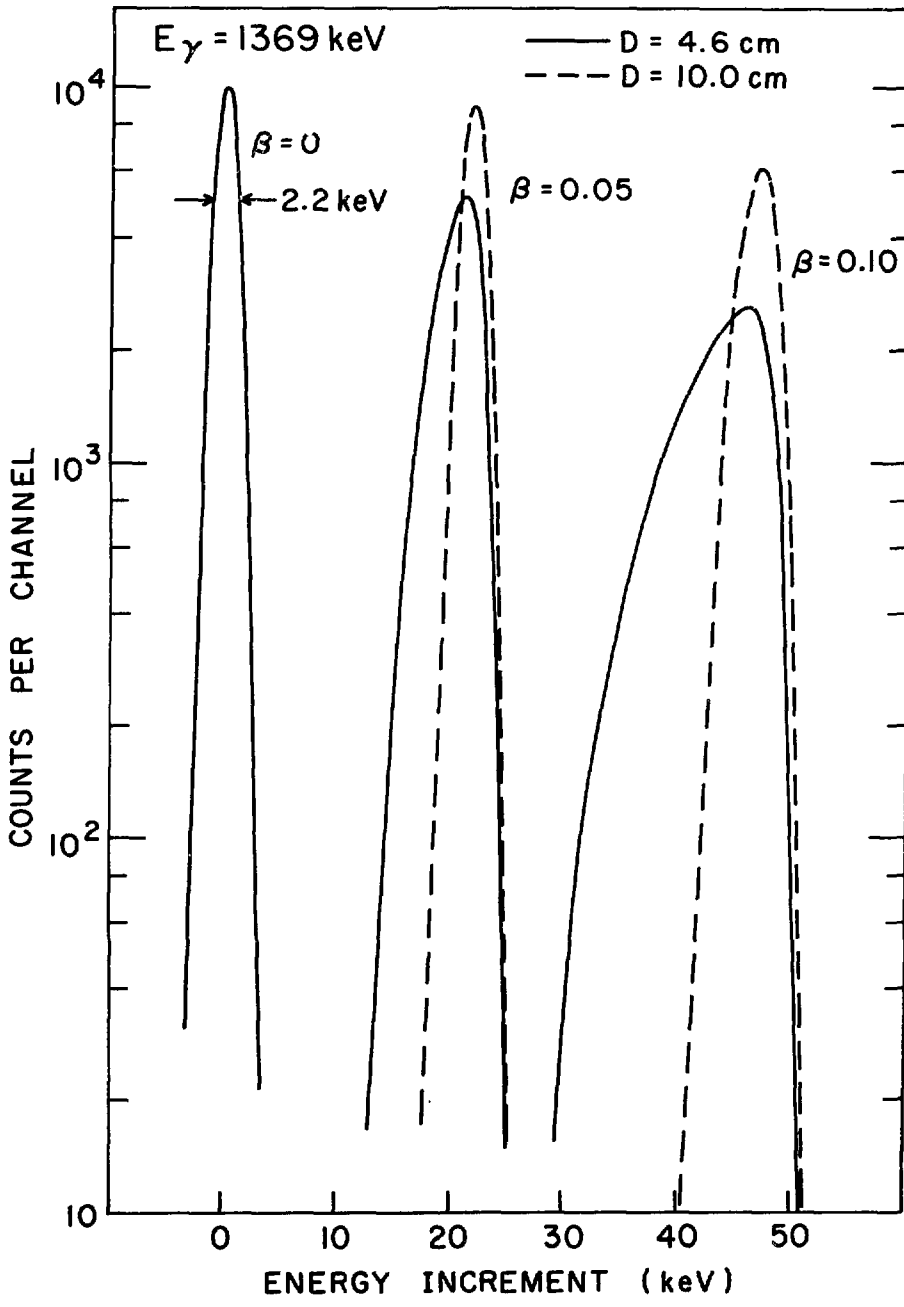


Figure 6

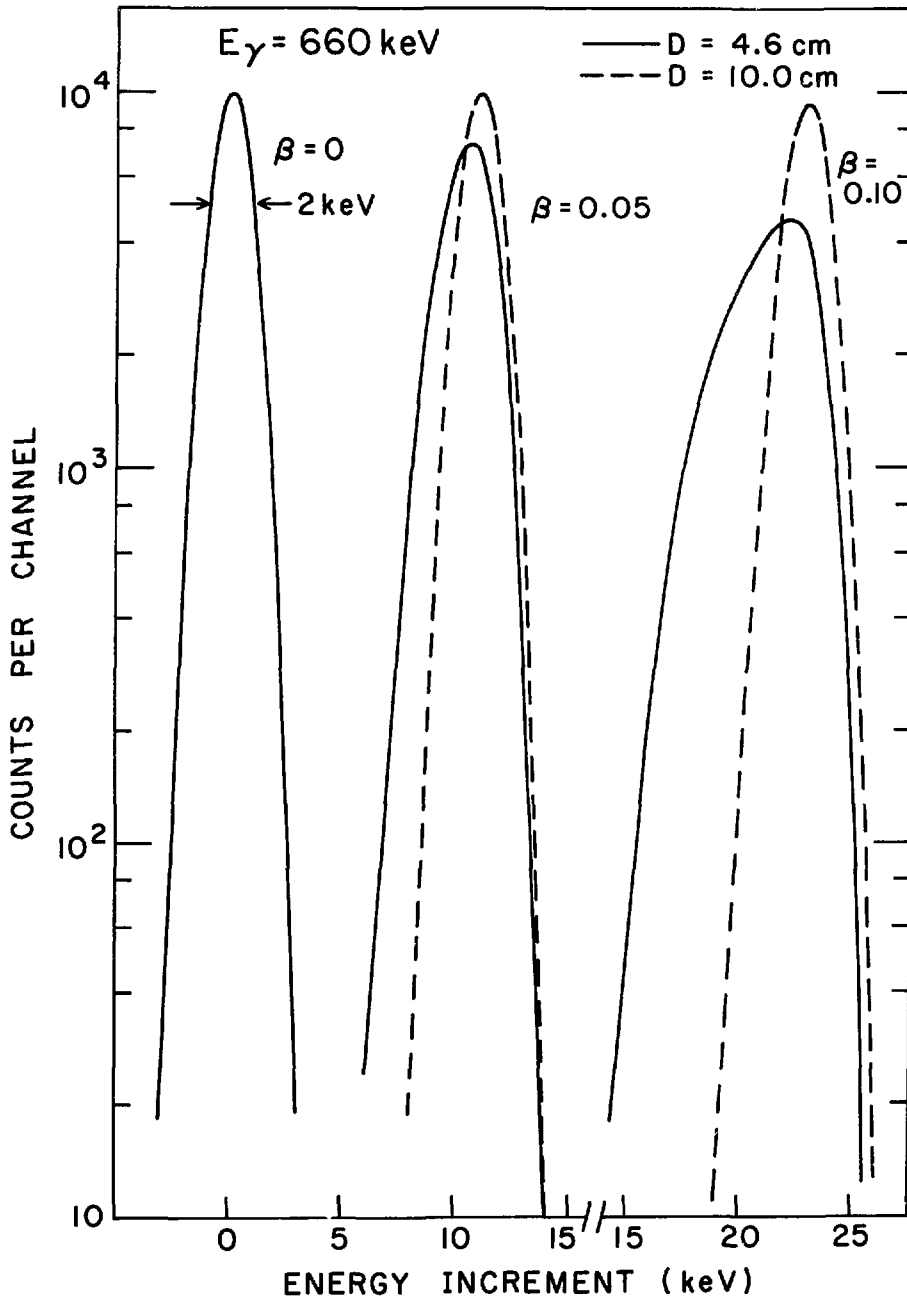


Figure 7



ISSN 0067 - 0367

To identify individual documents in the series we have assigned an AECL- number to each.

Please refer to the AECL- number when requesting additional copies of this document

from

Scientific Document Distribution Office
Atomic Energy of Canada Limited
Chalk River, Ontario, Canada
K0J 1J0

Price \$3.00 per copy

ISSN 0067 - 0367

Pour identifier les rapports individuels faisant partie de cette série nous avons assigné un numéro AECL- à chacun.

Veuillez faire mention du numéro AECL- si vous demandez d'autres exemplaires de ce rapport

au

Service de Distribution des Documents Officiels
L'Energie Atomique du Canada Limitée
Chalk River, Ontario, Canada
K0J 1J0

Prix \$3.00 par exemplaire